Improved Spike-based BMI Using Bayesian Adaptive Kernel Smoother and Deep Learning

Nur Ahmadi[1,2,4,5*]**, Trio Adiono**[4]**, Ayu Purwarianti**[4,5]**, Timothy G. Constandinou**[1,2,3]**, and Christos-Savvas Bouganis**[2]

[1]Centre for Bio-Inspired Technology, Imperial College London, London, SW7 2AZ, UK
[2]Department of Electrical and Electronic Engineering, Imperial College London, London, SW7 2AZ, UK
[3]Care Research & Technology Centre, UK Dementia Research Institute at Imperial College London
[4]School of Electrical Engineering and Informatics, Bandung Institute of Technology, Bandung, 40132, Indonesia
[5]Center for Artificial Intelligence (U-CoE AI-VLB), Bandung Institute of Technology, Bandung, 40132, Indonesia
[*]Corresponding author (n.ahmadi16@imperial.ac.uk)

SUPPLEMENTARY INFORMATION

**Suplementary Table 1.** Statistical description of monkey I neural data.

No	Recording session	Duration	Number of SUA	Number of MUA	Days since implantation
1	indy_20160407_02	13.63	114	90	29
2	indy_20160411_01	15.89	120	89	33
3	indy_20160418_01	22.63	136	91	40
4	indy_20160419_01	8.73	142	92	41
5	indy_20160420_01	25.89	147	91	42
6	indy_20160426_01	29.37	170	92	48
7	indy_20160622_01	40.83	155	94	105
8	indy_20160624_03	8.33	149	92	107
9	indy_20160627_01	56.05	156	91	110
10	indy_20160630_01	24.39	90	88	113
11	indy_20160915_01	6.35	135	88	190
12	indy_20160916_01	7.53	131	88	191
13	indy_20160921_01	6.00	135	88	196
14	indy_20160927_04	6.49	130	87	202
15	indy_20160930_02	7.68	133	90	205
16	indy_20161005_06	6.23	116	78	210
17	indy_20161006_02	8.37	133	87	211
18	indy_20161007_02	8.19	133	84	212
19	indy_20161011_03	11.23	139	91	216
20	indy_20161013_03	8.62	117	83	218
21	indy_20161014_04	8.65	142	90	219
22	indy_20161017_02	8.26	123	84	222
23	indy_20161024_03	7.87	125	77	229
24	indy_20161025_04	8.40	140	89	230
25	indy_20161026_03	8.29	120	84	231
26	indy_20161027_03	9.65	136	87	232
27	indy_20161206_02	12.30	111	90	272
28	indy_20161207_02	7.42	126	83	273
29	indy_20161212_02	9.35	108	85	278
30	indy_20161220_02	9.61	99	80	286
31	indy_20170123_02	10.16	109	92	320
32	indy_20170124_01	9.83	130	91	321
33	indy_20170127_03	12.23	123	94	324
34	indy_20170131_02	13.60	128	95	328

**Suplementary Table 2.** Statistical description of monkey L neural data.

No	Recording session	Duration	Number of SUA	Number of MUA	Days since implantation
1	loco_20170210_03	29.47	103	91	338
2	loco_20170213_02	40.29	120	94	341
3	loco_20170214_02	53.32	130	95	342
4	loco_20170215_02	18.67	114	92	343
5	loco_20170216_02	44.75	118	94	344
6	loco_20170217_02	30.68	124	94	345
7	loco_20170227_04	33.60	168	92	355
8	loco_20170228_02	29.68	165	90	356
9	loco_20170301_05	19.32	181	93	357
10	loco_20170302_02	38.06	165	90	358

Suplementary Table 3. Hyperparameter configuration of SUA-driven DL decoders across firing rate estimation algorithms.

| Hyperparameter	SUA-MLP			SUA-LSTM			SUA-QRNN		
	Binning	FKS	BAKS	Binning	FKS	BAKS	Binning	FKS	BAKS
Number of timesteps	1	1	1	2	2	2	3	4	4
Number of layers	2	2	2	1	1	1	1	1	1
Number of units	150	200	200	200	250	250	600	600	600
Number of epochs	8	5	5	6	9	9	3	15	12
Batch size	96	64	64	32	96	32	96	32	64
Dropout rate	0.2	0.2	0.2	0.4	0.5	0.1	0.4	0.4	0.5
Learning rate	0.0047	0.0049	0.0054	0.0120	0.0164	0.0103	0.0121	0.0071	0.0069
Optimiser	RMSProp	RMSProp	RMSProp	RMSProp	RMSProp	RMSProp	RMSProp	Adam	Adam
Number of parameters	40202	63602	63602	252402	365502	365502	413402	413402	413402
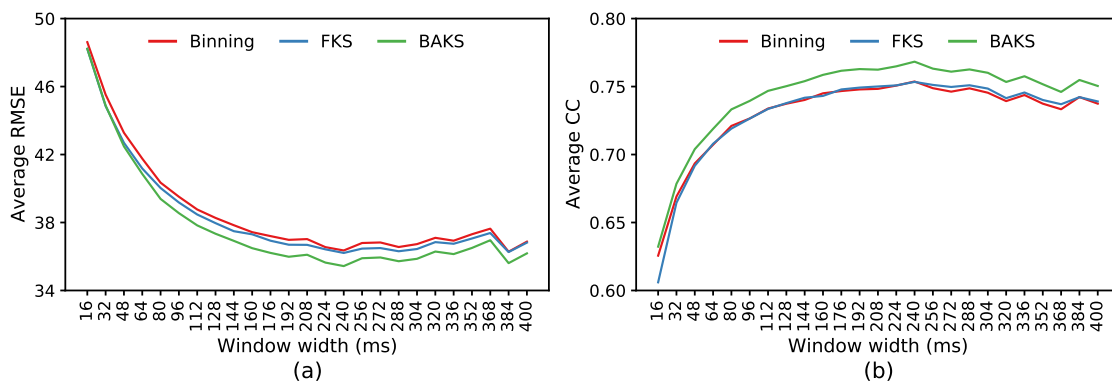
Suplementary Figure 1. Decoding performance comparison using MUA-driven KF decoder across different firing rate estimation algorithms with varying window widths. Performance comparison measured in (a) RMSE and (b) CC. Performance comparison used the validation sets of the first session I20160407_02.
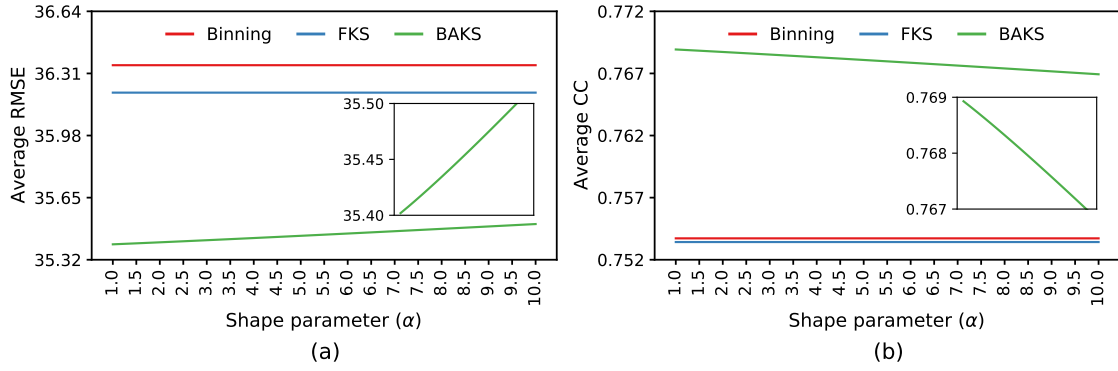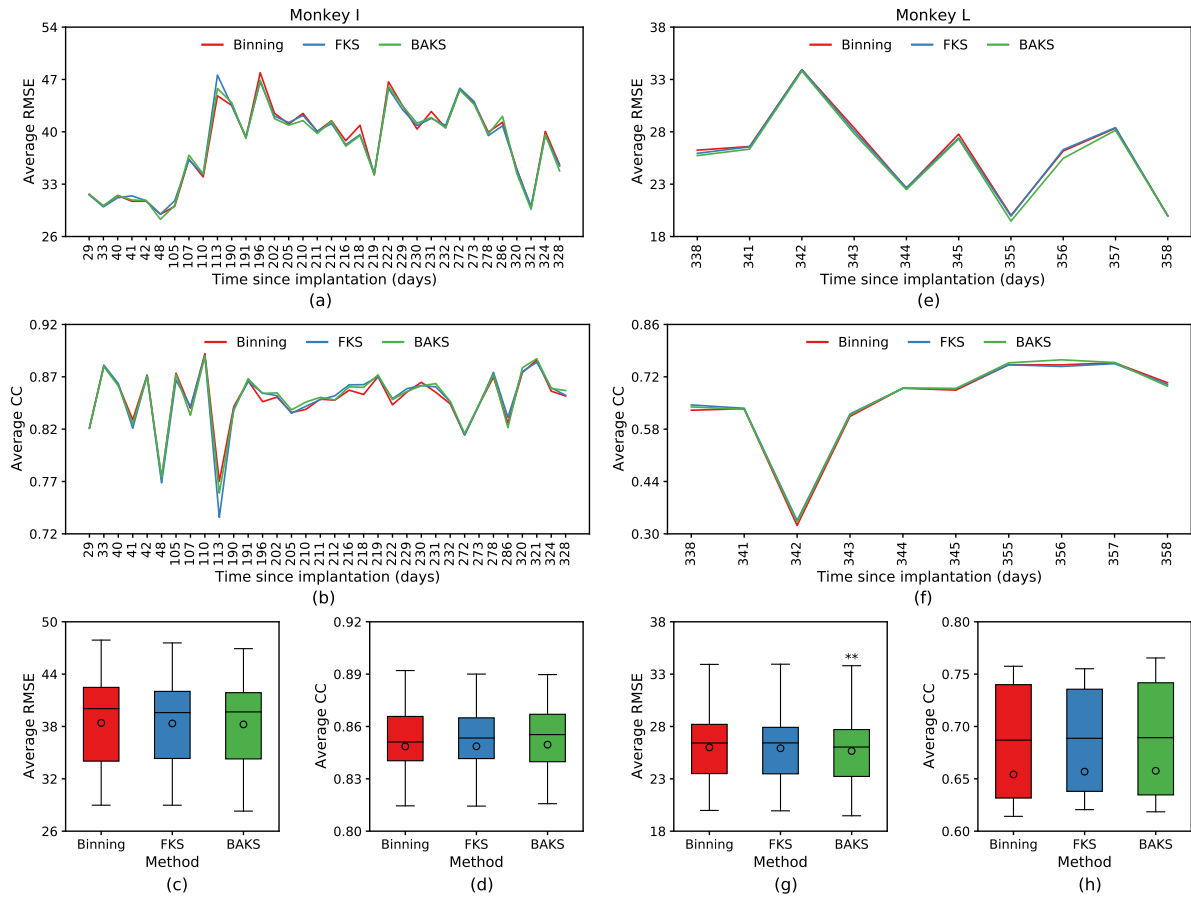
Suplementary Figure 2. Comparison of BAKS decoding performance using MUA-driven KF decoder under varying values of shape parameter (α). Performance comparison measured in (a) RMSE and (b) CC. The insets show the zoom-in views of BAKS decoding performance. Performance comparison used the validation sets of the first session I20160407_02.
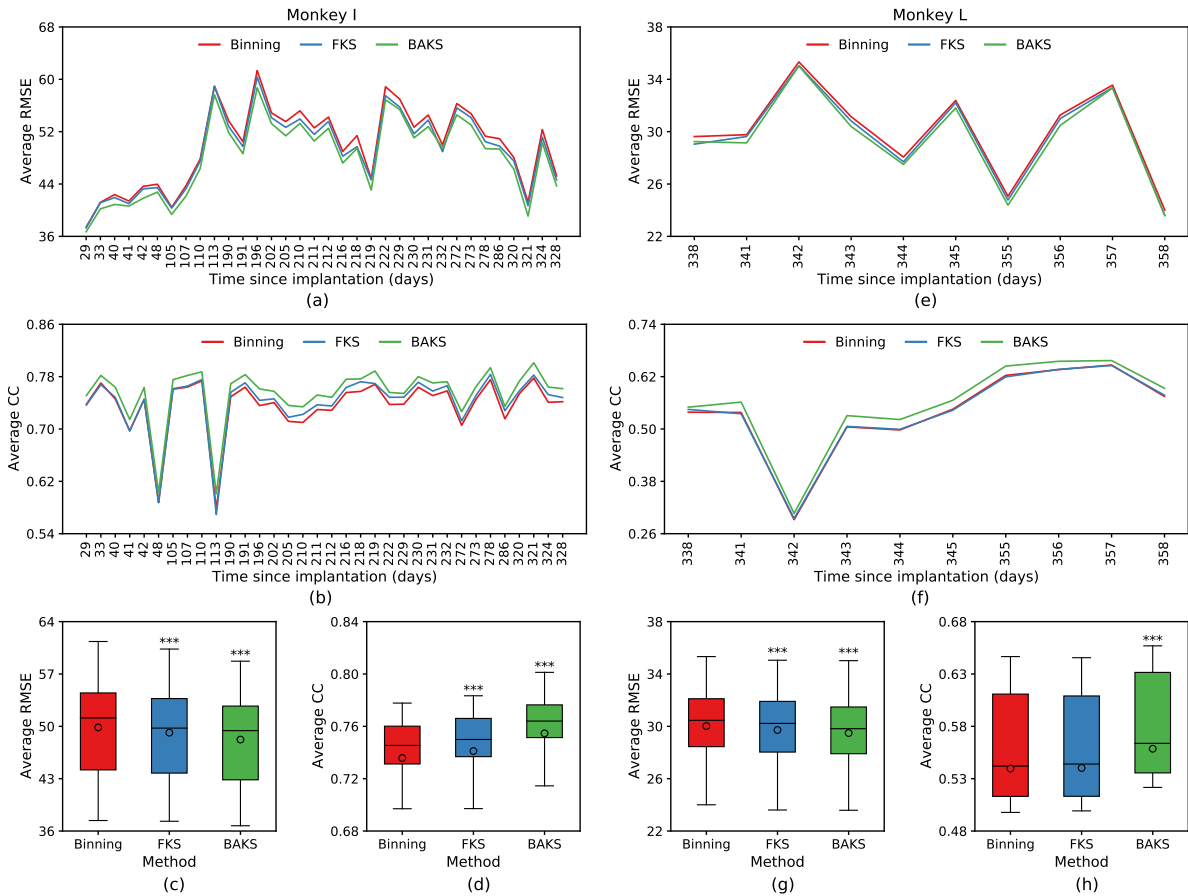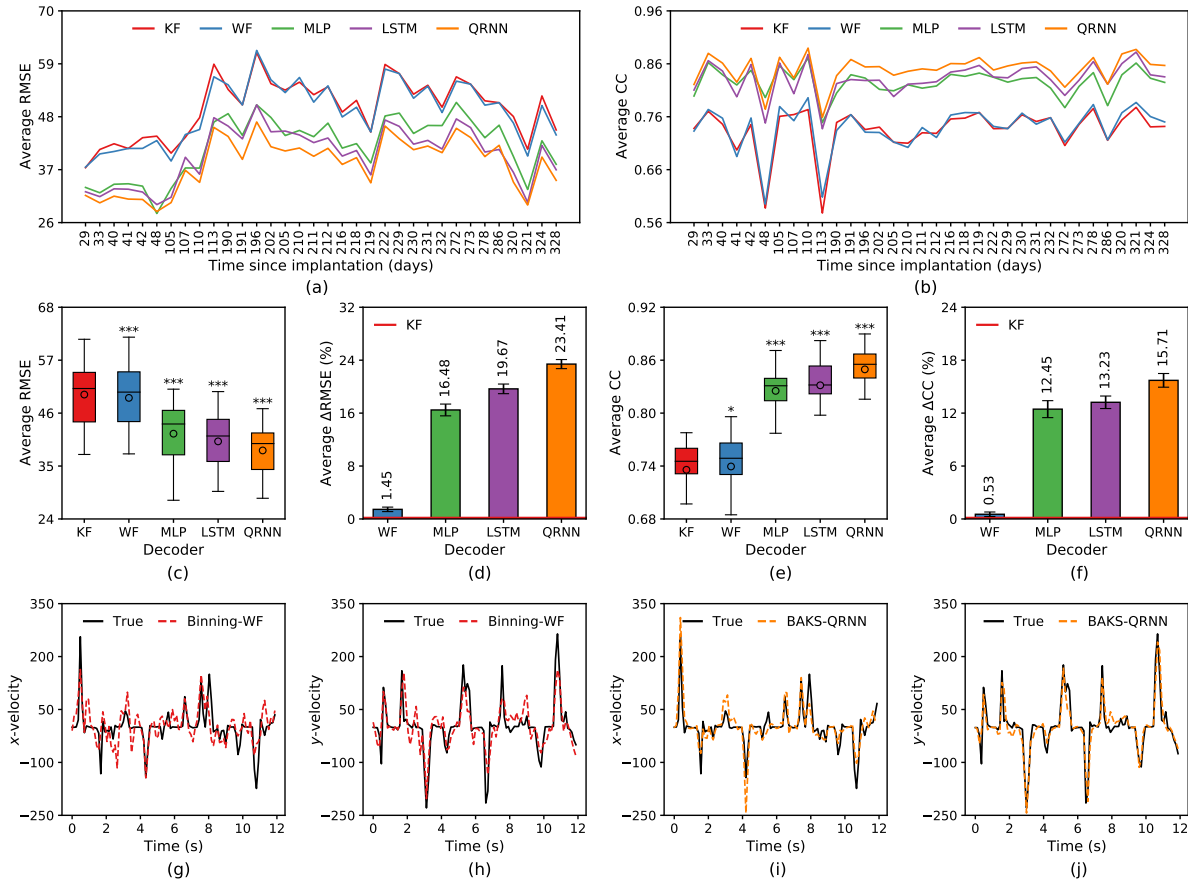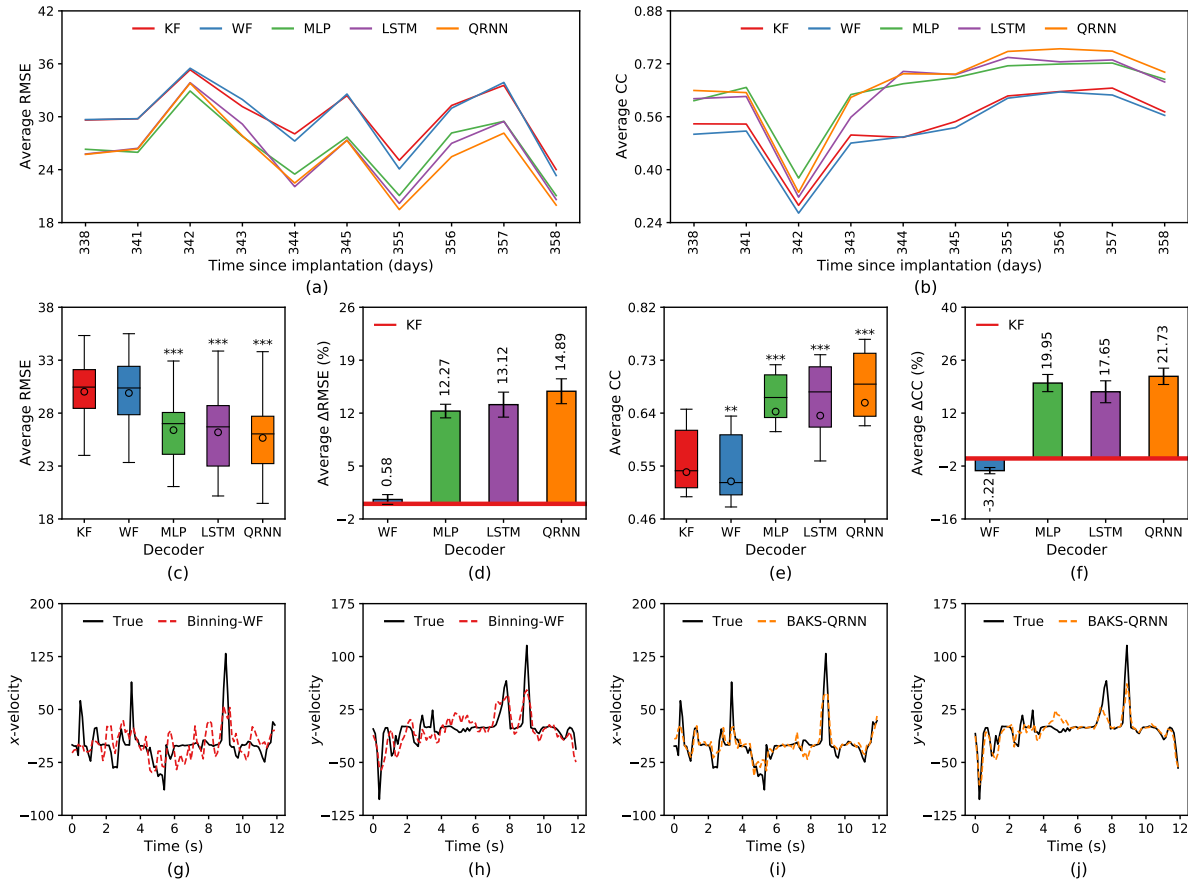

Suplementary Figure 3. Comparison of decoding performance of MUA-driven KF decoder across different firing rate estimation algorithms in monkeys I and L. (a),(b) Performance comparison across 34 recording sessions of monkey I measured in RMSE and CC, respectively. (c),(d) Boxplot comparison across 34 recording sessions of monkey I measured in RMSE and CC, respectively. (e),(f) Performance comparison across 10 recording sessions of monkey L measured in RMSE and CC, respectively. (c),(d) Boxplot comparison across 10 recording sessions of monkey L measured in RMSE and CC, respectively. Asterisks indicate firing rate estimation algorithms whose performances differ significantly from that of binning (** p<0.01, *** p<0.001).
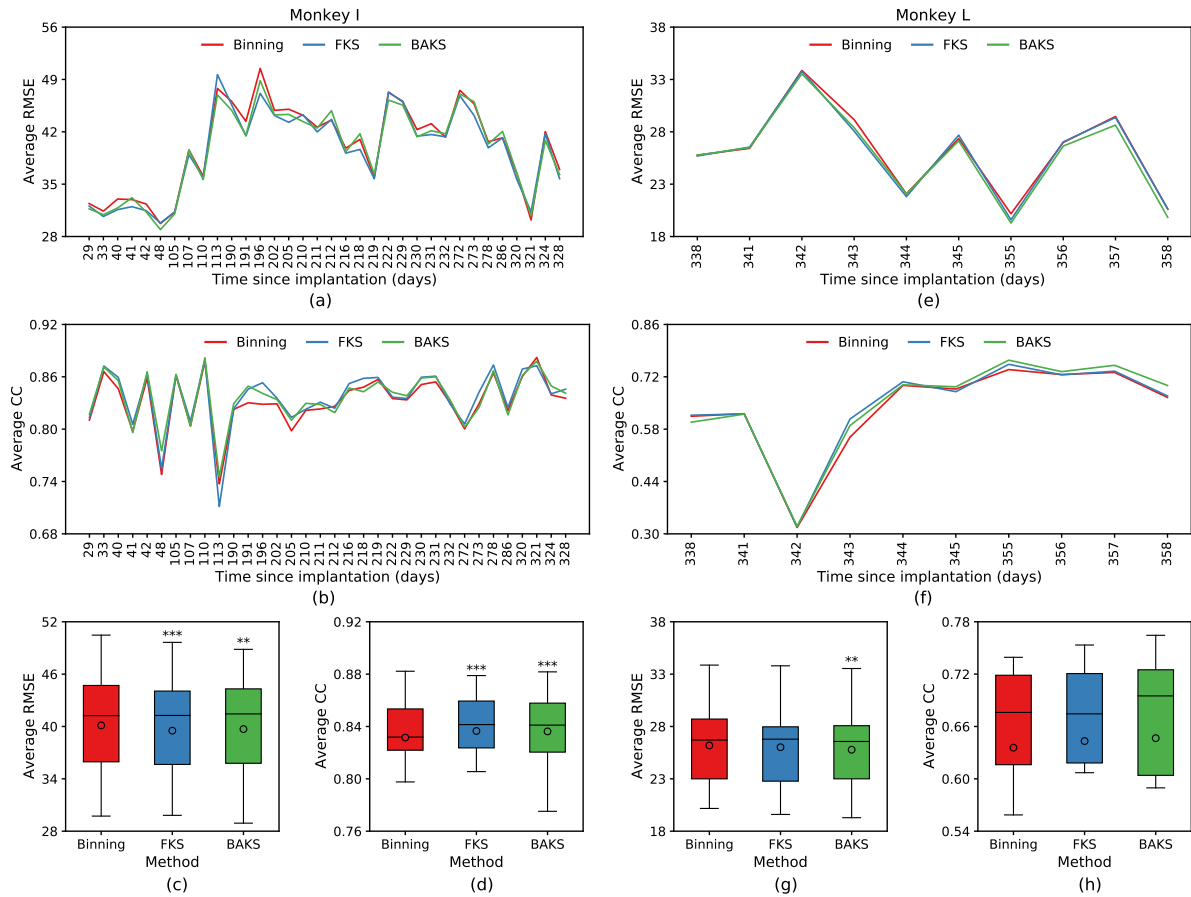
Suplementary Figure 4. Comparison of decoding performance of MUA-driven LSTM decoder across different firing rate estimation algorithms in monkeys I and L. (a),(b) Performance comparison across 34 recording sessions of monkey I measured in RMSE and CC, respectively. (c),(d) Boxplot comparison across 34 recording sessions of monkey I measured in RMSE and CC, respectively. (e),(f) Performance comparison across 10 recording sessions of monkey L measured in RMSE and CC, respectively. (c),(d) Boxplot comparison across 10 recording sessions of monkey L measured in RMSE and CC, respectively. Asterisks indicate firing rate estimation algorithms whose performances differ significantly from that of binning (** p<0.01, *** p<0.001).
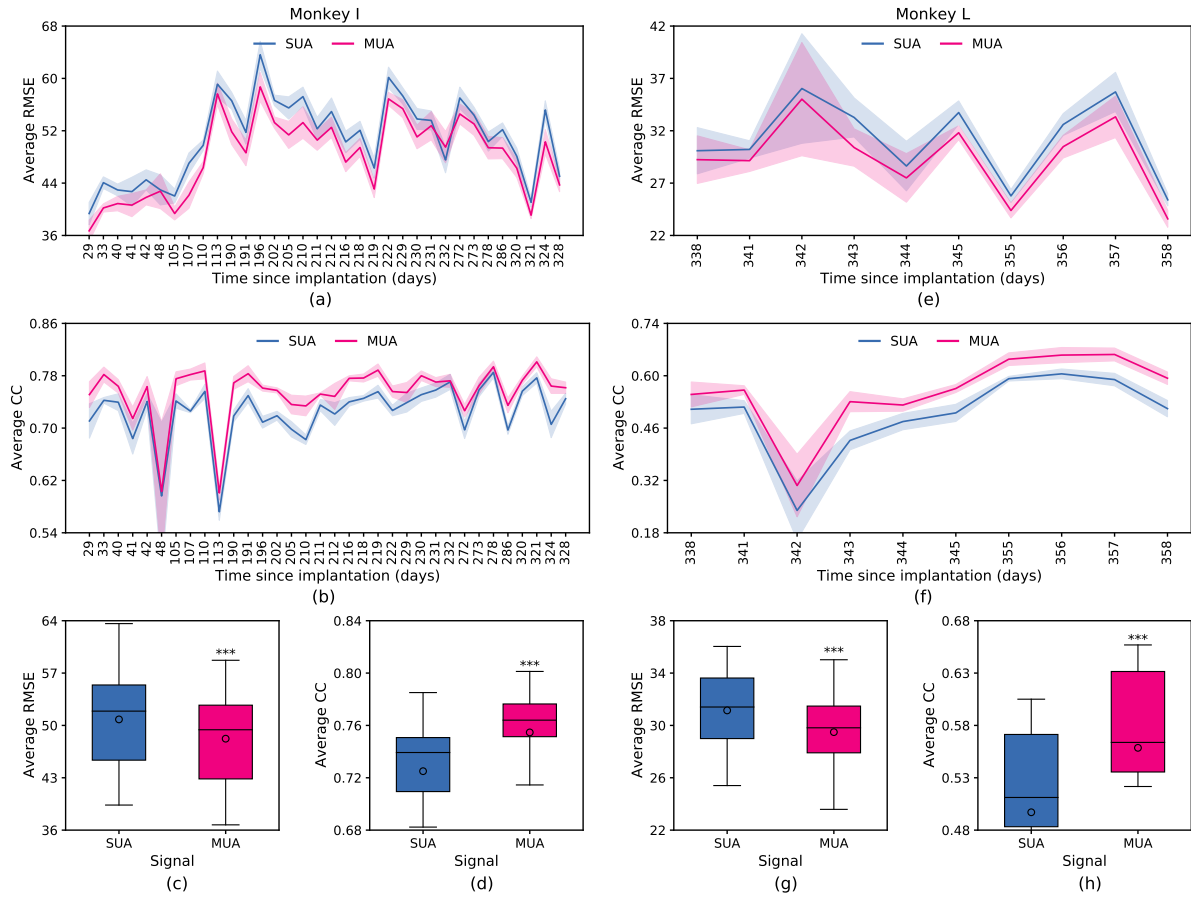
Suplementary Figure 5. Comparison of decoding performance of MUA-driven QRNN decoder across different firing rate estimation algorithms in monkeys I and L. (a),(b) Performance comparison across 34 recording sessions of monkey I measured in RMSE and CC, respectively. (c),(d) Boxplot comparison across 34 recording sessions of monkey I measured in RMSE and CC, respectively. (e),(f) Performance comparison across 10 recording sessions of monkey L measured in RMSE and CC, respectively. (c),(d) Boxplot comparison across 10 recording sessions of monkey L measured in RMSE and CC, respectively. Asterisks indicate firing rate estimation algorithms whose performances differ significantly from that of binning (** p<0.01, *** p<0.001).

Suplementary Figure 6. Decoding performance comparison between the proposed method (MUA-driven BAKS-QRNN decoder) and other decoders from monkey I dataset. Other decoders use binning for firing rate estimation. (a),(b) Performance comparison across 34 recording sessions of monkey I measured in RMSE and CC, respectively. (c),(e) Boxplot comparison across 34 recording sessions measured in RMSE and CC, respectively. Asterisks indicate decoders whose performances differ significantly from that of binning-KF decoder (* p<0.05, *** p<0.001). (d),(f) Performance improvement/degradation (in percent RMSE and CC, respectively) relative to binning-KF decoder. Positive (negative) value indicates performance improvement (degradation). Black error bars denote the standard error of the mean. (g)-(j) Snippet examples of true and decoded velocities in *x*- and *y*- coordinates from different decoders which are taken from the last recording session (I20170131_02).
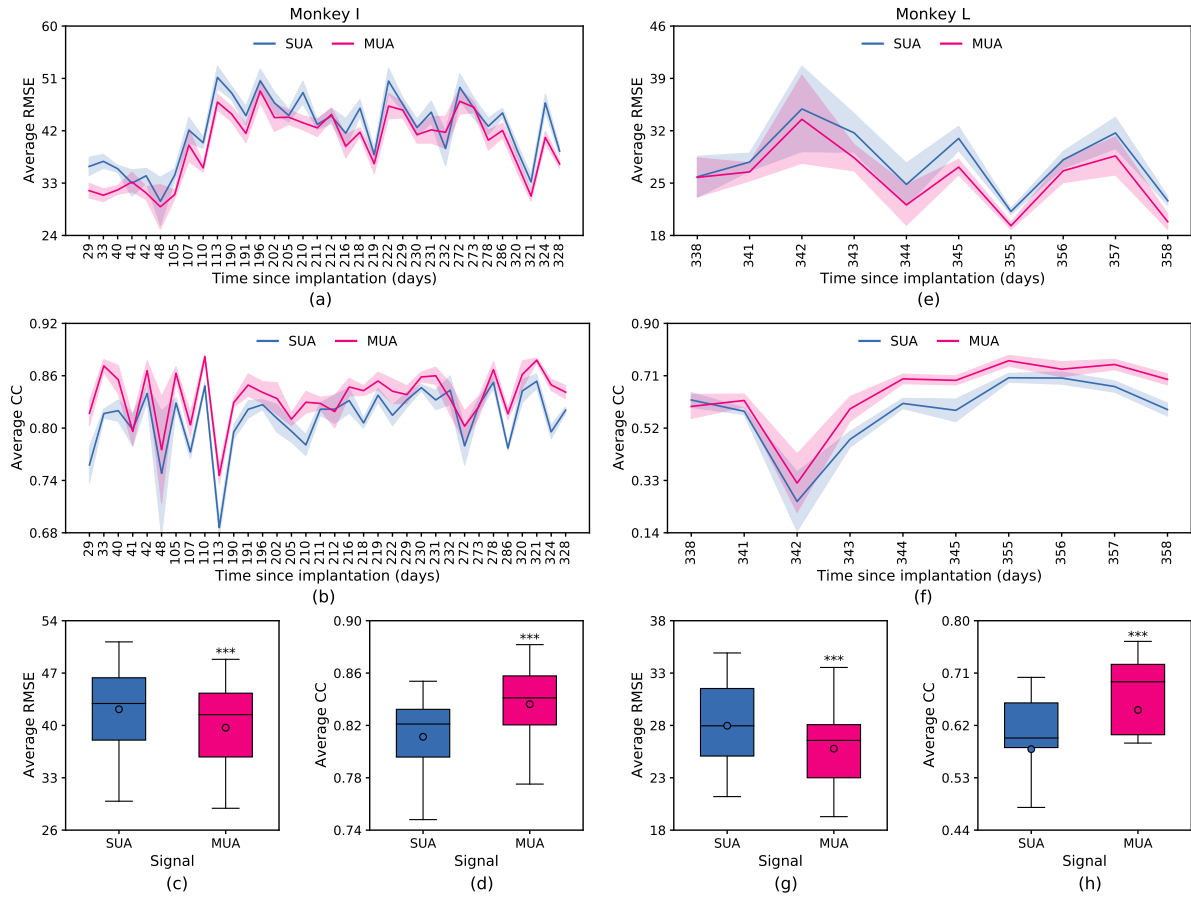
Supplementary Figure 7. Decoding performance comparison between the proposed method (MUA-driven BAKS-QRNN decoder) and other decoders from monkey L dataset. Other decoders use binning for firing rate estimation. (a),(b) Performance comparison across 10 recording sessions of monkey I measured in RMSE and CC, respectively. (c),(e) Boxplot comparison across 10 recording sessions measured in RMSE and CC, respectively. Asterisks indicate decoders whose performances differ significantly from that of binning-KF decoder (** p<0.01, *** p<0.001). (d),(f) Performance improvement/degradation (in percent RMSE and CC, respectively) relative to binning-KF decoder. Positive (negative) value indicates performance improvement (degradation). Black error bars denote the standard error of the mean. (g)-(j) Snippet examples of true and decoded velocities in *x*- and *y*- coordinates from different decoders which are taken from the last recording session (L20170302_02).

Suplementary Figure 8. Comparison of decoding performance between SUA and MUA using BAKS-KF decoder in monkeys I and L. (a),(b) Performance comparison across 34 recording sessions of monkey I measured in RMSE and CC, respectively. (c),(d) Boxplot comparison across 34 recording sessions of monkey I measured in RMSE and CC, respectively. (e),(f) Performance comparison across 10 recording sessions of monkey L measured in RMSE and CC, respectively. (c),(d) Boxplot comparison across 10 recording sessions of monkey L measured in RMSE and CC, respectively. Asterisk indicates that MUA yields statistically significant different in decoding performance compared to that of SUA (*** p<0.001).

Suplementary Figure 9. Comparison of decoding performance between SUA and MUA using BAKS-LSTM decoder in monkeys I and L. (a),(b) Performance comparison across 34 recording sessions of monkey I measured in RMSE and CC, respectively. (c),(d) Boxplot comparison across 34 recording sessions of monkey I measured in RMSE and CC, respectively. (e),(f) Performance comparison across 10 recording sessions of monkey L measured in RMSE and CC, respectively. (c),(d) Boxplot comparison across 10 recording sessions of monkey L measured in RMSE and CC, respectively. Asterisk indicates that MUA yields statistically significant different in decoding performance compared to that of SUA (*** p<0.001).